Efficient and Selectable Production of Reactive Species Using a Nanosecond Pulsed Discharge in Gas Bubbles in Liquid

Xiujuan J. Dai,* Cormac S. Corr, Sri B. Ponraj, Mohammad Maniruzzaman, Arun T. Ambujakshan, Zhiqiang Chen, Ladge Kviz, Robert Lovett, Gayathri D. Rajmohan, David R. de Celis, Marion L. Wright, Peter R. Lamb, Yakov E. Krasik, David B. Graves, William G. Graham, Riccardo d'Agostino, Xungai Wang
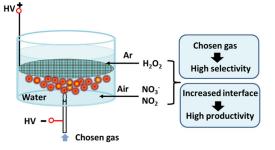
A plasma gas bubble-in-liquid method for high production of selectable reactive species using a nanosecond pulse generator has been developed. The gas of choice is fed through a hollow needle in a point-to-plate bubble discharge, enabling improved selection of reactive species. The increased interface reactions, between the gas-plasma and water through bubbles, give higher productivity. H_2O_2 was the predominant species produced using Ar plasma, while predominantly NO_3^- and NO_2 were generated using air plasma, in good agreement with the observed emission spectra. This method has nearly 100% selectivity for H_2O_2, with seven times higher production, and 92% selectivity for NO_3^-, with nearly twice the production, compared with a plasma above the water.

X. J. Dai, S. B. Ponraj, M. Maniruzzaman, A. T. Ambujakshan, Z. Chen, L. Kviz, R. Lovett, G. D. Rajmohan, D. R. de Celis, M. L. Wright, P. R. Lamb, X. Wang
Institute for Frontier Materials, Deakin University, Geelong Waurn Ponds, Victoria 3216, Australia
E-mail: jane.dai@deakin.edu.au
C. S. Corr
Research School of Physics and Engineering, Australian National University, Canberra 2601, Australia
Y. E. Krasik
Department of Physics, Technion, Haifa 32000, Israel
D. B. Graves
Department of Chemical and Biomolecular Engineering, University of California, Berkeley, California 94720, USA
W. G. Graham
Centre for Plasma Physics, School of Mathematics and Physics, Queen's University, Belfast BT7 1NN, UK
R. d'Agostino
University Aldo Moro of Bari, Bari 70126, Italy

1. Introduction

Reactive oxygen and nitrogen species (RONS), particularly hydrogen peroxide (H_2O_2), and nitrate ions (NO_3^-), can be generated by plasma in a liquid using an electric discharge.[1,2] These two liquid phase RONS generated by plasma have many potential applications in areas such as biomedicine,[1] nanoscience,[3] and agriculture.[4,5] Various discharge setups, including electrodes immersed in liquid and/or above liquid, and their effect on hydrogen peroxide yield have previously been examined.[6] The physics of these discharges and the plasma-induced chemistry have been studied to determine the underlying mechanisms.[3,7] As electrical breakdown in water requires a stronger electric field than in gas, gas bubbles have been externally introduced between submerged electrodes to reduce the required breakdown threshold. These discharges have been investigated by electrical characterization and emission

spectroscopy.[8–12] However, selectivity for the desired reactive species and efficient production of the required species are still key challenges.

In order to tailor the process for specific applications (e.g., milk sterilization or improved plant growth) this research has focused on: (1) enhancing the interface reaction between gas plasma and liquid, as the interface plays a critical role in controlling chemical reactions, and (2) achieving a selectable and controllable level of the required reactive species. A plasma gas bubble-in-liquid method with chosen gas was developed. Using different gases gives different gas phase reactive species enabling selective production of the required oxygen or nitrogen species. Due to the large difference in the dielectric constants of water ($e_r = 80$) and gas (e.g., air, $e_r = 1$), the electric field is enhanced in gas bubbles leading to plasma discharge formation at those locations. Through the bubbles (size, number, and movement), the interface reactions between the gas-plasma and water are increased enabling higher production of selected species.

2. Experimental Section

The experimental setup is shown in Figure 1a (called setup I). This setup has a hollow needle in a point-to-plate (mesh) electrode assembly with the gas flowing through the needle. Plasma was observed inside the bubbles when nanosecond duration high-voltage pulses were applied. The pulses were produced by a high voltage pulse generator FPM 15-10MC2 (FID GmbH). The generator can generate positive and negative pulses with the maximum of up to $+/-$ 15kV into 75 ohm, rise time of 2 ns and the duration of about 10 ns at 90% of maximum voltage. Here, we used $+9$ kV to the anode mesh electrode and -9 kV to the cathode needle electrode. The inner diameter of the needle was 0.44 mm. Gas flow rate was 100 sccm and the volume of deionized water was 100 mL.

For comparison, an electrode above water setup (called setup II, see Figure 1b) was examined. It consisted of a 50 mm diameter spiral top electrode covered by glass (2 mm above the water surface) with a similarly sized gas showerhead 10 mm above the electrode. The bottom mesh electrode was in the water, as in setup I, and the same water volume, frequency, applied voltage, and treatment

time were used. The spiral electrode, with the gas showerhead, was designed to increase the area of the interface between gas discharge and water. In these experiments either argon (inert gas) or air was used between the spiral electrode and the water surface. This setup allows generation of a plasma above the water surface by dielectric barrier discharge.

The treatment time and frequency were varied for each setup and gas. At least three separate trials were made for each condition and the concentration of the resultant species measured. The error bars in Figure 2 show the standard deviation of the measurements.

The concentration of hydrogen peroxide was measured using a titanium sulfate colorimetric method with a UV-Vis spectrophotometer examining absorbance spectra at 407 nm. Nitrate, nitrite, and ozone were measured by photometric assay (commercially available test kits, Spectroquant NOVA 60, Merck) at 525, 525, and 550 nm. The pH and the conductivity of treated de-ionized (DI) water were measured by a TPS WP-81 pH and conductivity meter. An ICCD camera was used to capture the formation of the plasma discharge, and a spectrometer to obtain emission spectra. The voltage applied across the electrode gap was measured using a high-voltage probe (Tektronix, P6015A) connected to the upper electrode, while the current was measured using an IonPhysics current probe across a 50 ohm termination.

3. Results and Discussion

It was found that, for Ar gas, the plasma in setup I produced a much higher density of H_2O_2, while for air the plasma produced a higher density of nitrogen dioxide and nitrate ions. As expected, "air" plasma also produced a much higher density of ozone, as well as a much higher conductivity but lower pH, than "argon" plasma. As H_2O_2 and NO_3^- are the most important products, only results for these two species are presented (see Figure 2).

Using Ar gas, the most reactive species in the plasma (energetic electrons, excited Ar atoms and ions, UV radiation) directly interact with water, which results in decomposition of the water and generation of OH radicals. Hydrogen peroxide is then formed by the recombination of OH radicals either in gas phase or in water. Due to the
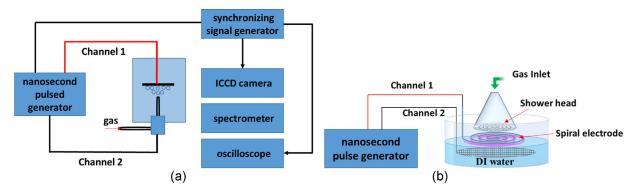

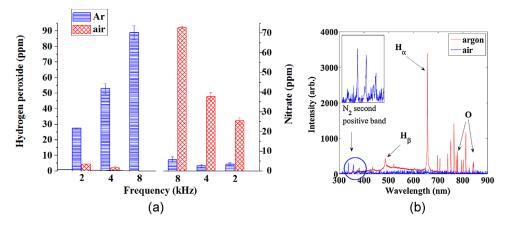**Figure 1.** Schematic of the experimental setup I (a) and setup II (b).

Figure 2. (a) The densities of H_2O_2 and NO_3^- generated in de-ionized (DI) water in Ar and air plasmas for 2 min at 2, 4 and 8 kHz; (b) Optical emission spectra of "argon" and "air" plasma in liquid at 4 kHz. The inset is an expanded view of the nitrogen second positive band observed with the air plasma.

bubble movement, H_2O_2 molecules are rapidly transferred into the bulk water enabling a high density to be achieved.

Using air, N and O are generated. They combine in the plasma to form nitric oxide (NO) in the gas phase, which readily combines with oxygen to form nitrogen dioxide (NO_2). Nitrogen dioxide is well known to disproportionate in H_2O forming NO_3^-, NO and H^+ as:

$$3NO_2 + 3H_2O \rightleftarrows 2NO_3^- + NO + 2H_3O^+ \tag{1}$$

Again due to the bubble movement, NO_2 rapidly diffuses into the bulk water so that a high density of NO_3^- and an acid solution is achieved, which was quantified by pH measurement. Figure 2a also shows that higher frequency operation of the pulsed generator results in higher densities of H_2O_2 in "Ar" plasma and higher densities of NO_3^- in "air" plasma. As more ozone was generated at higher average delivered power in "air" plasma, less H_2O_2 was found in the treated water. Very little ozone was found in "Ar" plasma treated water.

These results are in good agreement with the observed emission spectra. Figure 2b shows that "Ar" plasma generates a high intensity of hydrogen and oxygen species while the "air" plasma spectrum is dominated by the second positive band of nitrogen between 300 and 400 nm. These results strongly support the high selectivity of this method.
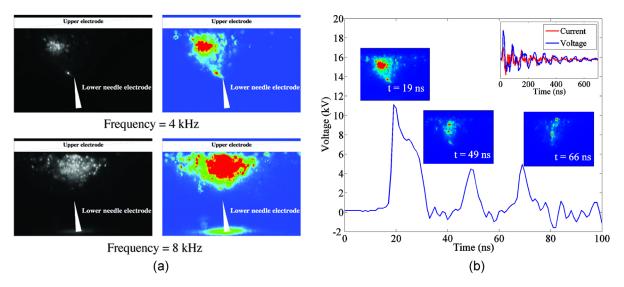
The energy efficiency of the production of radicals can be calculated for each species as the amount (n) produced divided by the energy consumption (E) for the process, i.e., n/E, where the value of E is equal to the product of the average power (P) and the treatment time (t). For the typical conditions described in the setup I (Experimental Section) at 4 kHz, the average power $P = 8.2 \times 10^{-4}$ kW (calculated from the current and voltage measurements (see inset, Figure 3b). With 2 min treatment, the energy input is $E = 2.7 \times 10^{-5}$ kWh. As ppm and mg/l are equivalent,

multiplying by 100 mL (the DI water volume used) then dividing by 10^6, gives the production in g. The energy efficiency under these conditions is then about 140 g/kWh for NO_3^- and 200 g/kWh for H_2O_2. The H_2O_2 production at lower power input is one to two orders higher than seen in the data summarized by Locke and Shih in their review paper.[6]

For a comparison of the selectivity and productivity between electrodes immersed in liquid and/or above liquid, setup II (plasma above water) was examined. With the same water volume, applied voltage and treatment time at 4 kHz, Table 1 shows that setup I gives much higher selectivity and production.

Setup I has 96% selectivity for H_2O_2 (using Ar gas instead of air) and 92% for NO_3^- (using air instead of Ar gas), and seven times higher production of H_2O_2 and nearly twice the production of NO_3^-, relative to setup II. In "Ar" plasma, NO_3^- production might come from residual air still present in setup II, although Ar gas was used to flush the system before the discharge was initiated. In "air" plasma, H_2O_2 production might result from ozone decomposition which allows additional sources for OH free radicals to form H_2O_2. These could contribute to the poorer selectivity of setup II. The lower production of reactive species of setup II can be explained by the reduced interface between gas plasma and water in setup II. The species produced in the gas plasma of setup II might also have recombined before diffusing into the water.

The visible light emission from the plasma discharge of both "Ar" and "air" plasmas was captured by a PIMAX 4 ICCD camera with 3 ns frame duration and 3 ns gate delay with respect to the beginning of the applied voltage for setup I. The light emission from the plasma was observed between the lower needle electrode and the upper mesh electrode. The dynamics of plasma formation was captured spatially and temporally through the discharge pulse. Figure 3a shows the "Ar" plasma light emission at 4 and

Figure 3. (a) Black and white image and color image of the plasma bubbles at 4 and 8 kHz at 19 ns in "Ar" plasma; (b) Images of the plasma dynamics through the high voltage pulse (determined at the generator) for a 4 kHz discharge and (inset) the current and voltage waveforms measured by probes during the discharge.

8 kHz at the maximum of the high-voltage pulse. The diameter of the bubbles prior to plasma initiation was about 2–3 mm. However, when the pulsed voltage was applied, intense light emission was obtained from locations with typical sizes of only ∼0.5 mm. A higher frequency leads to enhanced bubble fragmentation. This suggests that significant enhancement of the electric field at the tip of the needle electrode leads to strong and spatially non-uniform water polarization. The latter results in "squeezing" of the gas bubbles, causing them to break up into smaller bubbles.[13] The smaller and greater density of bubbles in the liquid, the larger the surface area of the gas-water interface for a given volume. The increased interface reactions between gas-plasma and water will give faster transport from plasma to liquid so that more of the reactive species can diffuse into the liquid. This contributes to the higher production of reactive species. In addition, the bubble movement will also ensure rapid mixing.

Although the duration of the applied voltage produced by the pulse generator was only ∼10 ns, it was found that the light emission from the plasma lasted for nearly

500 ns. Figure 3b shows plasma dynamics through the high voltage pulse. It can be seen that the peak in plasma emission intensity is observed at the maximum of the high-voltage pulse. Plasma light emission at longer exposures can be explained by oscillations observed in the current and voltage waveforms (inset Figure 3b), due to non-matched conditions between the pulse generator impedance and the load, and to recombination processes having typical times of several hundreds of nanoseconds. This may actually contribute to the high production of reactive species.

The selectivity and higher production of the reactive species can benefit specific applications. For example, the selectivity for H_2O_2 improves the potential of plasma sterilization of milk,[14] the higher production of nitrates is promising for generating fertilizers for plant growth while H_2O_2 stimulates plant growth,[15] and the controllable level of the reactive species in plasma water provides a non-toxic electrolyte for nanomaterial fabrication.[16]

4. Conclusion

An improved method, using gas bubbles in liquid with choice of gas, was demonstrated for higher productivity and selectivity of desired reactive species. "Ar" plasma can be used to produce a high concentration of H_2O_2, while "air" plasma can be used to produce high concentrations of NO_3^- and NO_2. The increased interface reactions between gas-plasma and water with fast mass transport from plasma to liquid, due to smaller and more numerous bubbles, enables

Table 1. Comparison between Setup I and Setup II of H_2O_2 and NO_3^- concentrations generated in Ar and air plasmas.

Gas	H_2O_2 (ppm)		NO_3^- (ppm)	
	Setup I	Setup II	Setup I	Setup II
Ar	53	7	3	13
Air	2	11	38	20

higher production of reactive species. The improved productivity and selectivity of reactive species can benefit specific applications.

[1] D. B. Graves, *J. Phys. D: Appl. Phys.* **2012**, *45*, 263001.

[2] J. L. Brisset, E. Hnatiuc, *Plasma Chem. Plasma Process.* **2012**, *32*, 655.

[3] W. G. Graham, K. R. Stalder, *J. Phys. D: Appl. Phys.* **2011**, *44*, 174037.

[4] D. P. Park, K. Davis, S. Gilani, C. A. Alonzo, D. Dobrynin, G. Friedman, A. Fridman, A. Rabinovich, G. Fridman, *Curr. Appl. Phys.* **2013**, *13*, S19–S29.

[5] A. Lindsay, B. Byrns, W. King, A. Andhvarapou, J. Fields, D. Knappe, W. Fonteno, S. Shannon, *Plasma Chem. Plasma Process.* **2014**, *34*, 1271.

[6] B. R. Locke, K. Y. Shih, *Plasma Sources Sci. Technol.* **2011**, *20*, 034006.

[7] P. Bruggeman, C. Leys, *J. Phys. D: Appl. Phys.* **2009**, *42*, 053001.

[8] P. Vanraes, A. Nikiforov, C. Leys, *J. Phys. D: Appl. Phys.* **2452**, *45*, 06.

[9] S. Gershman, O. Mozgina, A. Belkind, K. Becker, E. Kunhardt, *Contrib. Plasma Phys.* **2007**, *47*, 19.

[10] H. Aoki, K. Kitano, S. Hamaguchi, *Plasma Sources Sci. Technol.* **2008**, *17*, 025006.

[11] J. Sidney Clements, M. Sato, R. H. Davis, *IEEE Trans. Ind. Appl.* **1987**, *1A-23*, 2.

[12] B. S. Sommers, J. E. Foster, *Plasma Sources Sci. Technol.* **2014**, *23*, 015020.

[13] C. G. Garton, Z. Krasucki, *Proc. R. Soc. Lond. Ser. A Math. Phys. Eng. Sci* **1964**, *280*, 211.

[14] S.B. Ponraj, J. Sharp, J.R. Kanwar, A.J. Sinclair, L. Kviz, K.R. Nicholas, X.J. Dai, ISPC 22, Belgium, July, **2015**.

[15] M. Maniruzzaman, H.I. Hussain, X. Wang, A. Sinclair, D.M. Cahill, X.J. Dai, ISPC 22, Belgium, July, **2015**.

[16] T.A. Arun, A.Z. Sadek, S.B. Ponraj, G.D. Rajmohan, M. Maniruzzaman, Z.Q. Chen, A. Sullivan, J.M. Pringle, C.S. Corr, J. du Plessis, X.J. Dai, ISPC 22, Belgium, July, **2015**.